

Reactions of the Heavier Group 14 Element Alkyne Analogues Ar'EEAr' ($\text{Ar' = C}_6\text{H}_3\text{-2,6(C}_6\text{H}_3\text{-2,6-Pr}^i_2)_2$; E = Ge, Sn) with Unsaturated Molecules: Probing the Character of the EE Multiple Bonds

Chunming Cui, Marilyn M. Olmstead, James C. Fetting, Geoffrey H. Spikes, and Philip P. Power*

Contribution from the Department of Chemistry, University of California Davis, One Shields Avenue, Davis, California 95616

Received August 16, 2005; E-mail: pppower@ucdavis.edu

Abstract: Reactions of the alkyne analogues Ar'EEAr' ($\text{Ar' = C}_6\text{H}_3\text{-2,6(C}_6\text{H}_3\text{-2,6-Pr}^i_2)_2$; $\text{E = Ge (1); Sn (2)}$) with unsaturated molecules are described. Reaction of **1** and **2** with azobenzene afforded the new hydrazine derivatives $\text{Ar'E}\{(\text{Ph})\text{NN}(\text{Ph})\}\text{EA}'$ ($\text{E = Ge (3); Sn (4)}$). Treatment of **1** with Me_3SiN_3 gave the cyclic singlet diradicaloid $\text{Ar'Ge}\{\mu_2\text{-(NSiMe}_3)_2\}\text{GeAr'}$ (**5**), whereas **2** afforded the monoimide bridged $\text{Ar'Sn}\{\mu_2\text{-N(SiMe}_3)\}\text{-SnAr'}$ (**6**). Reaction of **1** with $t\text{-BuNC}$ or PhCN yielded the adduct $\text{Ar'GeGe(CNBu)}\text{Ar'}$ (**7**) or the ring compound $\text{Ar'Ge-N(Ph)CC(Ph)N-GeAr'}$ (**8**). In contrast, the tin compound **2** did not react with either $t\text{-BuNC}$ or PhCN . Treatment of **1** with $\text{N}_2\text{CH(SiMe}_3)$ generated $\text{Ar'Ge}\{\mu_2\text{-CH(SiMe}_3)\}\{\mu_2\text{:}\eta^2\text{-N}_2\text{CH(SiMe}_3)\}\{\mu_2\text{-N}_2\text{-CH(SiMe}_3)\}\text{GeAr'}$ (**9**) which contains ligands in three different bridging modes and no Ge—Ge bonding. Reaction of **1** with an excess of N_2O gave a germanium peroxo species $\text{Ar'(HO)Ge}(\mu_2\text{-O})(\mu_2\text{:}\eta^2\text{-O}_2)\text{Ge-(OH)Ar'}$ (**10**) which features a Ge—O—Ge—O—O ring. Oxidation of **1** by tetracyanoethylene (TCNE) led to cleavage of the Ge—Ge bond and formation of a large multiring system of formula $\text{Ar'Ge}^{3+}\{(\text{TCNE})^{2-}\}_3\text{-(GeAr')}_3^+$. The digermynes **1** also reacted with 1 equiv of $\text{Ph}\equiv\text{CPh}$ to give the 1,2-digermacyclobutadiene **12**, which has a Ge—C—C—Ge ring, and with $\text{Me}_3\text{SiC}\equiv\text{CH}$ or $\text{PhC}\equiv\text{C-C}\equiv\text{CPh}$ to activate a flanking $\text{C}_6\text{H}_3\text{-2,6-Pr}^i_2$ ring and give the tricyclic products **13** and **14**. The “distannyne” **2** did not react with these acetylenes. Overall, the experiments showed that **1** is highly reactive toward unsaturated molecules, whereas the corresponding tin congener **2** is much less reactive. A possible explanation of the reactivity differences in terms of the extent of the singlet diradical character of the Ge—Ge and Sn—Sn bonds is discussed.

Introduction

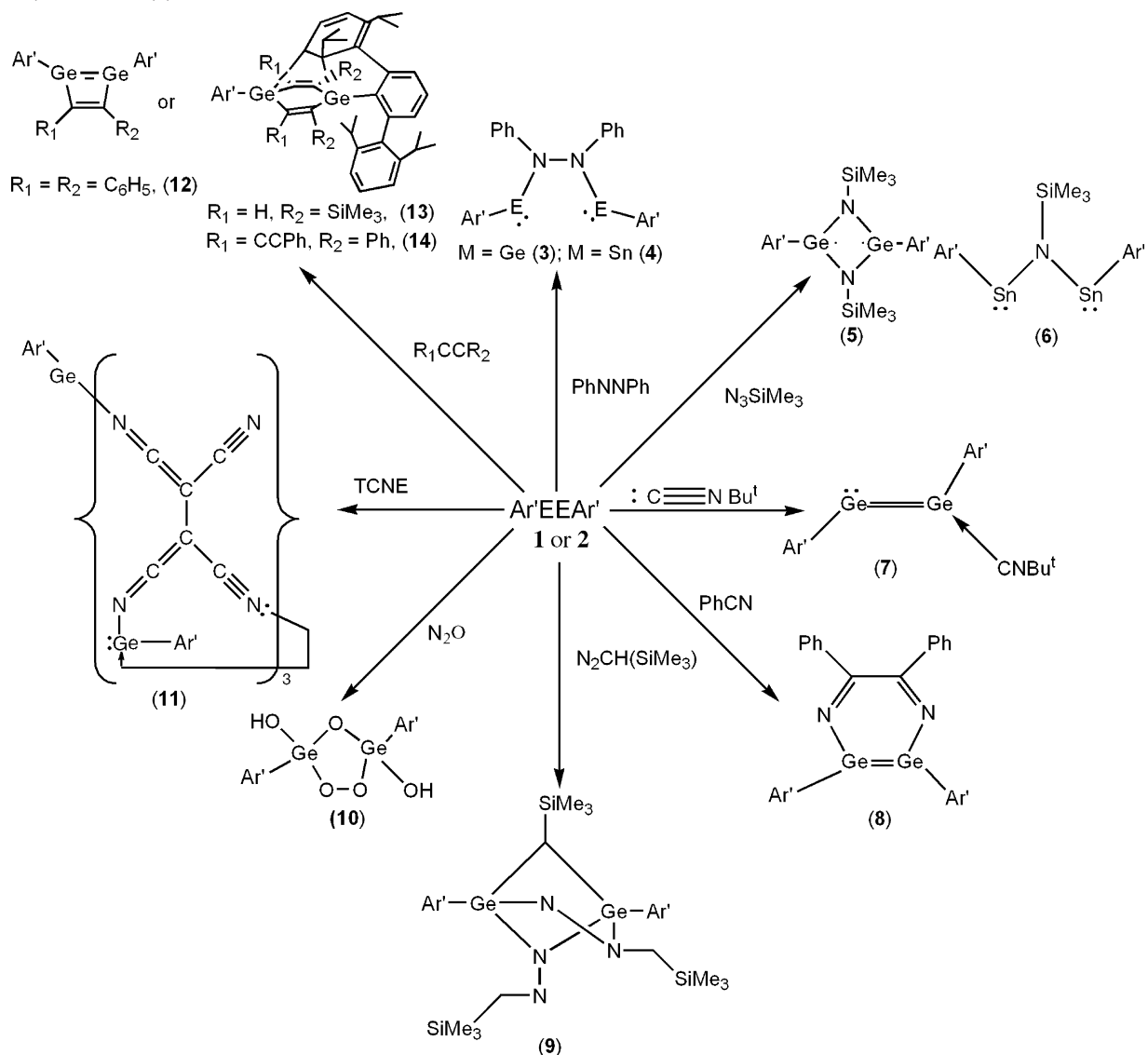
Stable heavier group 14 element multiply bonded species have attracted considerable attention over the last two decades because of their unusual bonding and structures.^{1–4} Despite the large number of theoretical calculations⁵ and attempts to synthesize them,⁶ stable heavier alkyne congeners REER (E = Si–Pb) remained unknown until recently.^{7–11} The structures^{8–11} of these compounds disclosed a trans-bent rather than linear geometry in which the R–M–M angle decreases from silicon to lead.

This trend indicates increasing lone pair character and decreasing E—E bond order upon descending the group, and this finding is well correlated with computational results.^{5,12} Few reactions of these compounds have been reported, however.¹³ It is highly desirable to explore their chemical reactivity in order to understand the bonding in these unique molecules. We have already described the synthesis and structures of the alkyne analogues of germanium⁹ and tin¹⁰ Ar'EEAr' ($\text{Ar' = C}_6\text{H}_3\text{-2,6(C}_6\text{H}_3\text{-2,6-Pr}^i_2)_2$; E = Ge (1), Sn(2)) as well as their reduction with alkali

- (1) Davidson, P. J.; Lappert, M. F. *Chem. Commun.*, **1973**, 317. (b) Goldberg, D. E.; Harris, D. H.; Lappert, M. F.; Thomas, K. M. *Chem. Commun.*, **1976**, 261.
- (2) West, R.; Fink, M. J.; Michl, J. *Science* **1981**, *214*, 1343.
- (3) Brook, A. G.; Abdesaken, F.; Gutekunst, B.; Gutekunst, G.; Kallury, R. K. *Chem. Commun.*, **1981**, 191.
- (4) (a) Tokitoh, N.; Okazaki, R. In *The chemistry of organic germanium tin and lead compounds*; Rapport, Z., Ed.; Wiley: Chichester, 2002; Vol. 2, Chapter 13. (b) Weidenbruch, M. *J. Organomet. Chem.* **2002**, *646*, 39. (c) Escudie, J.; Ranaivonjatovo, H. *Adv. Organomet. Chem.* **1999**, *44*, 113. (d) Power, P. P. *Chem. Rev.* **1999**, *99*, 3463.
- (5) (a) Karni, M.; Kapp, J.; Schleyer, P. v. R.; Apeloig, Y. In *The Chemistry of Organic Silicon Compounds*; Rapport, Z., Apeloig, Y., Eds.; Wiley: Chichester, 2002; Vol. 3, Chapter 1. (b) Ganzer, I.; Hartmann, M.; Frenking, G. In *The Chemistry of Organic Germanium Tin and Lead Compounds*; Rapport, Z., Ed.; Wiley: Chichester, 2002; Vol. 2, Chapter 3.

- (6) For example: (a) Sekiguchi, A.; Zigler, S. S.; West, R.; Michl, J. *J. Am. Chem. Soc.* **1986**, *108*, 4241. (b) Pietschnig, R.; West, R.; Powell, D. R. *Organometallics* **2000**, *19*, 2724. (c) Wiberg, N.; Finger, C. M. M.; Polborn, K. *Angew. Chem., Int. Ed.* **1993**, *32*, 1054. (d) Karni, M.; Apeloig, Y.; Schroeder, D.; Zummack, W.; Rabzanna, R.; Schwartz, H. *Angew. Chem., Int. Ed. Engl.* **1999**, *38*, 332.
- (7) Power, P. P. *Chem. Commun.* **2003**, 2091.
- (8) Pu, L.; Twamley, B.; Power, P. P. *J. Am. Chem. Soc.* **2000**, *122*, 3524.
- (9) Stender, M.; Phillips, A. D.; Wright, R. J.; Power, P. P. *Angew. Chem., Int. Ed.* **2002**, *41*, 1785.
- (10) Phillips, A. D.; Wright, R. J.; Olmstead, M. M.; Power, P. P. *J. Am. Chem. Soc.* **2002**, *124*, 5930.
- (11) Sekiguchi, A.; Kinjo, R.; Ichinohe, M. *Science* **2004**, *305*, 1755.
- (12) Grev, R. S. *Adv. Organomet. Chem.* **1991**, *33*, 125. (b) Nagase, S.; Kobayashi, K.; Takagi, N. *J. Organomet. Chem.* **2000**, *611*, 264. (c) Takagi, N.; Nagase, S. *Eur. J. Inorg. Chem.* **2002**, 2775.
- (13) Stender, M.; Phillips, A. D.; Power, P. P. *Chem. Commun.* **2002**, 1312.

Scheme 1. Summary of Reactions Undergone by the Germanium and Tin Alkyne Analogues Ar'EEAr' (M = Ge, 1; Sn, 2; Ar' = C₆H₃-2,6(C₆H₃-2,6-Pr'₂)₂) with Unsaturated Molecules



metals to give the reduced ions $[Ar'EEAr']^-$ and $[Ar'EEAr']^{2-}$.^{14,15} The successful isolation of **1** and **2** in gram quantities has allowed us to study their reaction chemistry with a variety of species and has allowed insight into their electronic and structural properties as well as a comparison of their reaction patterns with the lighter alkynes. We have communicated the initial result that $Ar'GeGeAr'$ (**1**) could be added to alkynes in a [2+2] fashion to afford the first stable, formally antiaromatic cyclobutadiene analogue incorporating heavier main group 14 elements, i.e., 1,2-digerma-cyclobutadiene $Ar'Ge\{Ph\}CC(Ph)\}_2$.¹⁶ In addition we reported that **1** reacted with N_3SiMe_3 to liberate N_2 with formation of the diradicaloid, $Ar'Ge-$

$\{\mu_2-N(SiMe_3)\}_2GeAr'$,¹⁷ and have described briefly the high reactivity of these compounds.¹⁸ We now present a more extensive study of the reactivity of $Ar'EEAr'$ (E = Ge, Sn) toward a variety of unsaturated molecules (summarized in Scheme 1) and discuss the implications of our results for the MM bonding in these compounds.

Experimental Section

All operations were carried out by using modified Schlenk techniques under an atmosphere of dry argon or nitrogen. Solvents were dried over an alumina column and degassed prior to use. The chemicals used in this study were purchased from Aldrich or Acros and used as received. $Ar'EEAr'$ (M = Ge,⁹ Sn¹⁰) were prepared as described in the literature. The ¹H, ¹³C, ¹¹⁹Sn NMR spectroscopic data were recorded on Varian INOVA 300 or 400 MHz spectrometers. The ¹H and ¹³C NMR spectra were referenced to the deuterated solvent, and the ¹¹⁹Sn NMR spectra were externally referenced to $SnMe_4/C_6D_6$. UV-vis data were recorded on a Hitachi-1200 spectrometer.

(14) Pu, L.; Phillips, A. D.; Richards, A. F.; Stender, M.; Simons, R. S.; Olmstead, M. M.; Power, P. P. *J. Am. Chem. Soc.* **2003**, *125*, 11626.

(15) Singly and doubly reduced ionic species of formula $[Ar'MMAr']^{1-2-}$ (M = Ge or Sn; $Ar' = C_6H_3-2,6(C_6H_3-2,4,6-Pr'_2)_2$) having the related Ar' substituents were discovered before the neutral $Ar'EEAr'$ compounds. See: (a) Olmstead, M. M.; Simons, R. S.; Power, P. P. *J. Am. Chem. Soc.* **1997**, *119*, 11705. (b) Pu, L.; Senge, M. O.; Olmstead, M. M.; Power, P. P. *J. Am. Chem. Soc.* **1998**, *120*, 12682.

(16) Cui, C.; Olmstead, M. M.; Power, P. P. *J. Am. Chem. Soc.* **2004**, *126*, 5062.

(17) Cui, C.; Brynda, M.; Olmstead, M. M.; Power, P. P. *J. Am. Chem. Soc.* **2004**, *126*, 6510.

(18) Power, P. P. *Appl. Organomet. Chem.* **2005**, *19*, 488.

Ar'Ge{(Ph)NN(Ph)}GeAr' (3) and Ar'Sn{(Ph)NN(Ph)}SnAr' (4):

A mixture of Ar'GeGeAr' (0.152 g, 0.160 mmol) and PhNNPh (0.029 g, 0.160 mmol) in *n*-hexane (10 mL) was stirred at room temperature for 16 h. The solvent volume was reduced to ca. 3 mL under reduced pressure. Storage at -20°C for 2 days afforded orange crystals of **3** (0.140 g, 78%). Mp: 147°C . ^1H NMR (C_6D_6 , 399.77 MHz) (all broad): δ 1.04 (d, $J = 6.8$ Hz, 48H, CHMe_2), 1.29 (d, $J = 6.8$ Hz, 24H, CHMe_2), 2.71 (sept., $J = 6.8$ Hz, 8H, CHMe_2), 6.90 (d, $J = 6.8$ Hz, 4H, *m*- C_6H_5), 6.97 (m, 4H, *m*- C_6H_5), 7.07 (d, $J = 8.0$ Hz, 4H, 8H, *m*-Dipp), 7.19 (m, 2H, *p*- C_6H_5), 7.27 (m, 6H, *p*-Dipp and *p*- C_6H_5), 8.18 (d, $J = 8.2$ Hz, 4H, *o*- C_6H_5). $^{13}\text{C}\{^1\text{H}\}$ NMR (C_6D_6 , 100.59 MHz): δ 24.90 (CHMe_2), 25.39 (CHMe_2), 30.93 (CHMe_2), 123.23 (*m*- C_6H_5), 123.91 (*m*-Dipp), 126.62 (*p*- C_6H_5), 129.18 (*p*- C_6H_5), 129.36 (*m*- C_6H_5), 131.02 (*i*- C_6H_5), 139.60 (*p*-Dipp), 144.99 (*i*-Dipp), 146.61 (*i*- C_6H_5), 153.10 (*o*- C_6H_5), 158.09 (*o*- C_6H_5). UV-vis (*n*-hexane): $\lambda = 521$ nm ($\epsilon = 2800$). In a similar manner, reaction of Ar'SnSnAr' (0.17 g, 0.165 mmol) and azobenzene (0.030 g, 0.165 mmol) in toluene at room temperature for 16 h, followed by recrystallization from *n*-hexane at -20°C , afforded orange crystals of **4** (0.128 g, 64%). Mp: 164°C . ^1H NMR (C_6D_6 , 399.77 MHz): δ 0.96 (d, $J = 6.8$ Hz, 6H, CHMe_2), 1.01 (d, $J = 6.8$ Hz, 12H, CHMe_2), 1.07 (d, $J = 6.8$ Hz, 6H, CHMe_2), 1.11 (d, $J = 6.8$ Hz, 6H, CHMe_2), 1.30 (d, $J = 6.8$ Hz, 6H, CHMe_2), 1.36 (d, $J = 6.8$ Hz, 6H, CHMe_2), 1.46 (d, $J = 6.8$ Hz, 6H, CHMe_2), 2.83 (m, 4H, CHMe_2), 3.37 (m, 4H, CHMe_2), 6.54 (t, $J = 7.2$ Hz, 2H, *p*-Dipp), 6.72 (t, $J = 7.2$ Hz, 2H, *p*-Dipp), 7.05 (t, $J = 7.2$ Hz, 2H, *p*- C_6H_5), 7.09 (m, 8H, *m*-Dipp), 7.22 (m, 10H, *m*- C_6H_5 , *m*- C_6H_5 and *p*- C_6H_5), 8.02 (d, $J = 7.2$ Hz, 4H, *o*- C_6H_5). ^{13}C NMR (C_6D_6 , 100.59 MHz): δ 21.58 (CHMe_2), 22.54 (CHMe_2), 24.36 (CHMe_2), 26.30 (CHMe_2), 26.75 (CHMe_2), 28.57 (CHMe_2), 31.01 (CHMe_2), 118.99, 123.06, 123.57, 124.24, 125.25, 128.69, 129.21, 129.62, 130.41, 130.81, 144.21, 145.62, 146.37, 147.37, 148.80, 153.25, 156.42, 158.08 (Ar-C). ^{119}Sn NMR (C_6D_6 , 149.00 MHz): δ 463.9. UV-vis (*n*-hexane): $\lambda = 486$ nm ($\epsilon = 1700$).

Ar'Ge $\{\mu_2\text{-N}(\text{SiMe}_3)\}_2\text{GeAr' (5) and Ar'Sn $\{\mu_2\text{-N}(\text{SiMe}_3)\}_2\text{SnAr' (6):$$

To a solution of **1** (0.100 g, 0.106 mmol) in *n*-hexane (3 mL) was added an excess of Me_3SiN_3 (0.073 g, 0.64 mmol). After the reaction mixture was stirred at room temperature for 48 h, it was stored at 5°C for 2 d to afford dark violet crystals of **5** (0.104 g, 88%). Mp: 145°C (dec). ^1H NMR (C_7D_8 , 399.77 MHz): δ -0.30 (s, 18H, SiMe_3), 0.91 (d, $J = 6.8$ Hz, 48H, CHMe_2), 1.18 (d, $J = 6.8$ Hz, 24H, CHMe_2), 2.75 (sept., $J = 6.8$ Hz, 8H, CHMe_2), 6.91 (m, 6H, Ar-H), 7.03 (m, 4H, *m*- C_6H_5), 7.10 (m, 12H, Ar-H). ^{13}C NMR (d_8 -toluene, 100.59 MHz): δ 5.15 (SiMe_3), 23.92 (CHMe_2), 26.34 (CHMe_2), 31.82 (CHMe_2), 123.21, 125.90, 128.43, 130.12, 137.12, 137.56, 138.75, 152.98, 172.45 (Ar-C). UV-vis (*n*-hexane): $\lambda = 521$ nm ($\epsilon = 6000$). In a similar manner, **2** (0.109 g, 0.106 mmol) in toluene (3 mL) was reacted with an excess of Me_3SiN_3 (0.073 g, 0.64 mmol). The solution was stirred at room temperature for 2 d and stored at ca. -20°C for 1 week to afford red crystals of **6** (0.075 g, 62.0%). Mp: 132°C . ^1H NMR (C_6D_6 , 399.77 MHz): δ -0.32 (s, 9H, SiMe_3), 0.99 (d, $J = 6.8$ Hz, 48H, CHMe_2), 1.18 (d, $J = 6.8$ Hz, 24H, CHMe_2), 3.11 (sept., $J = 6.8$ Hz, 8H, CHMe_2), 7.05 (m, 6H, Ar-H), 7.07 (m, 4H, Ar-H), 7.10 (m, 4H, Ar-H), 7.20 (m, 4H, Ar-H). $^{13}\text{C}\{^1\text{H}\}$ NMR (C_6D_6 , 100.59 MHz): δ 3.26 (SiMe_3), 21.74 (CHMe_2), 24.20 (CHMe_2), 29.18 (CHMe_2), 121.32, 125.74, 127.56, 130.38, 138.71, 137.18, 139.14, 154.62, 174.35 (Ar-C). ^{119}Sn NMR (C_6D_6 , 149.00 MHz): δ 907.1. UV-vis (*n*-hexane): $\lambda = 435$ nm ($\epsilon = 7000$).

Ar'GeGe(CNBu')Ar' (7):

To a solution of **1** (0.162 g, 0.134 mmol) in *n*-hexane (5 mL) was added neat *t*-BuNC (0.012 g, 0.14 mmol) at room temperature. The solution was stirred for 20 h and stored at -20°C for 1 week to give red dark crystals of **7** (0.065 g, 47%). Mp: 125°C (dec). ^1H NMR (C_6D_6 , 399.77 MHz) (all broad): δ 0.88 (s, 9H, *t*-Bu), 0.97 (m, 24H, CHMe_2), 1.22 (m, 12H, CHMe_2), 1.40 (m, $J = 6.8$ Hz, 12H, CHMe_2), 2.94 (m, 8H, CHMe_2), 6.94 (m, 8H, Ar-H), 7.18 (m, 8H, Ar-H). ^{13}C NMR (C_6D_6 , 100.59 MHz): δ 14.36 ($\text{C}\equiv\text{N}$),

23.06 (CHMe_2), 24.57 (CHMe_2), 25.74 (CHMe_2), 25.76 (CHMe_2), 29.18 (CMe_3), 30.86 (CMe_3), 30.90 (CHMe_2), 31.96 (CHMe_2), 123.29, 123.86, 123.90, 125.19, 126.89, 129.06, 129.25, 129.54, 129.91, 141.49, 144.49, 145.83, 146.88, 147.19, 147.65, 148.24 (Ar-C). UV-vis (*n*-hexane): $\lambda = 490$ nm ($\epsilon = 3000$). IR (KBr, Nujol): 2092 (m), CN stretch.

Ar'Ge{(Ph)CN(CN)(Ph)}GeAr' (8):

To a solution of **1** (0.124 g, 0.132 mmol) in *n*-hexane was added neat PhCN (0.028 g, 0.272 mmol). The mixture was stirred at room temperature for 3 days. The solvent was removed under reduced pressure, and the remaining red powder was crystallized from diethyl ether at -20°C to give orange crystals of **8** (0.077 g, 51.6%). Mp: 167°C (dec). ^1H NMR (C_6D_6 , 399.77 MHz): δ 0.96 (d, $J = 6.8$ Hz, 24H, CHMe_2), 1.23 (d, $J = 6.8$ Hz, 24H, CHMe_2), 2.75 (sept., $J = 6.8$ Hz, 8H, CHMe_2), 6.90 (m, 6H, Ar-H), 7.10 (m, 12H, Ar-H), 7.32 (m, 6H, Ar-H), 8.12 (d, 4H, C_6H_5). ^{13}C NMR (C_6D_6 , 100.59 MHz): δ 21.78 (CHMe_2), 25.36 (CHMe_2), 32.06 (CHMe_2), 122.90, 124.76, 125.87, 126.21, 130.26, 133.05, 136.42, 137.06, 138.02, 138.23, 148.67, 157.40, 169.38 (Ar-C). UV-vis (*n*-hexane): $\lambda = 421$ nm ($\epsilon = 4000$).

Ar'Ge $\{\mu_2\text{-}\eta^1\text{-CH}(\text{SiMe}_3)\}\{\mu_2\text{-}\eta^1\text{-N}_2\text{CH}(\text{SiMe}_3)\}\{\mu_2\text{-}\eta^2\text{-N}_2\text{CH}(\text{SiMe}_3)\}_2\text{GeAr' (9):$

To a solution of **1** (0.170 g, 0.181 mmol) in *n*-hexane (10 mL) was added $\text{N}_2\text{CHSiMe}_3$ (0.6 mL, 1 M solution in *n*-hexane, 0.60 mmol). The mixture was stirred at room temperature for 2 d, and the volume of the solution was reduced to ca. 3 mL under reduced pressure. The solution was stored at ca. -20°C for 1 week to give yellow crystals of **9** (0.127 g, 56.0%). Mp: 118°C (dec). ^1H NMR (C_6D_6 , 399.77 MHz): δ -0.09 (s, 9H, SiMe_3), -0.02 (s, 9H, SiMe_3), 0.12 (s, 9H, SiMe_3), (CHMe_2), 1.17 (d, $J = 6.8$ Hz, 24H, CHMe_2), 2.80 (sept., $J = 6.8$ Hz, 8H, CHMe_2), 6.90 (d, 4H, Ar-H), 7.10 (m, 8H, Ar-H), 7.21 (m, 2H, Ar-H), 7.30 (m, 4H, Ar-H). $^{13}\text{C}\{^1\text{H}\}$ NMR (C_6D_6 , 100.59 MHz): δ 20.94 (CHMe_2), 25.02 (CHMe_2), 30.76 (CHMe_2), 123.45, 124.09, 126.89, 130.16, 138.23, 143.40, 145.13, 147.09, 155.74 (Ar-C).

Ar'(HO)Ge($\mu_2\text{-O}$)($\mu_2\text{-}\eta^2\text{-O}_2$)Ge(OH)Ar' (10):

A solution of **1** (0.170 g, 0.181 mmol) in toluene (5 mL) was exposed to an N_2O atmosphere, causing the original red solution to become yellow immediately. The solution was stirred for 30 min, concentrated under reduced pressure, and stored at -20°C for 2 days to furnish colorless crystals of **10** (0.103 g, 57.5%). Mp: 127°C (dec). ^1H NMR (C_6D_6 , 399.77 MHz): δ 0.92 (d, $J = 6.8$ Hz, 24H, CHMe_2), 1.23 (d, $J = 6.8$ Hz, 24H, CHMe_2), 1.45 (s, 2H, OH), 2.91 (sept., $J = 6.8$ Hz, 8H, CHMe_2), 6.94 (d, 4H, Ar-H), 7.08 (m, 8H, Ar-H), 7.24 (m, 2H, Ar-H), 7.32 (m, 4H, Ar-H). ^{13}C NMR (C_6D_6 , 100.59 MHz): δ 20.72 (CHMe_2), 24.87 (CHMe_2), 30.26 (CHMe_2), 122.98, 123.79, 126.05, 130.00, 136.83, 140.28, 145.92, 147.12, 154.47 (Ar-C). IR (KBr, Nujol): 3621 (s), O-H stretch.

Ar'Ge[(NC) $_2$ CC(CN) $_2$](GeAr') $_3$ (11):

A mixture of **1** (0.170 g, 0.181 mmol) and tetracyanoethylene (0.035 g, 0.27 mmol) in toluene (10 mL) was stirred at room temperature for 3 d. The solvent was removed under reduced pressure, and the residue was dissolved in diethyl ether (15 mL). Storage at -20°C for 3 d afforded pale yellow crystals of **11**. Mp: 162°C . ^1H NMR (C_6D_6 , 399.76 MHz): δ 0.86 (d, $J = 6.8$ Hz, 12H, CHMe_2), 0.98 (m, 12H, CHMe_2), 1.08 (m, 12H, CHMe_2), 1.13 (m, 18H, CHMe_2), 1.25 (d, 12H, CHMe_2), 1.33 (m, 18H, CHMe_2), 1.45 (d, $J = 6.8$ Hz, 12H, CHMe_2), 2.38 (sept, 4H, $J = 6.6$ Hz, CHMe_2), 2.77 (sept, 4H, $J = 6.6$ Hz, CHMe_2), 2.97 (m, 8H, CHMe_2), 6.94 (m, 6H, Ar-H), 7.03 (m, 3H, Ar-H), 7.11 (m, 6H, Ar-H), 7.12 (d, 3H, Ar-H), 7.18–7.22 (m, 9H, Ar-H), 7.32–7.38 (m, 3H, Ar-H), 7.72 (m, 6H, Ar-H). $^{13}\text{C}\{^1\text{H}\}$ NMR (C_6D_6 , 100.52 MHz): δ 22.69, 23.31, 23.43, 23.60, 25.17, 25.24, 25.51, 25.58, 26.08 (CHMe_2), 30.90, 31.16, 31.22, 31.42 (CHMe_2), 122.47, 122.89, 123.00, 123.88, 124.60, 125.80, 129.40, 129.61, 129.73, 131.42, 132.04, 134.70, 134.82, 138.93, 139.00, 145.74, 146.48, 146.73, 147.21, 147.33, 147.50, 147.89, 149.62, 150.44.

Reaction with Alkynes; Synthesis of 12, 13, and 14.

A mixture of **1** (0.140 g, 0.149 mmol) and diphenylacetylene (0.053 g, 0.30 mmol) in *n*-hexane (30 mL) was stirred at room temperature for 7 d. The resulting deep red solution was concentrated and stored at 6°C

Table 1. X-ray Crystallographic Data for Compounds **3**, **4**, **6**, **7**, **8**, **9**, **10**, **11**, **14**

compd	3- <i>n</i> -hexane	4- <i>n</i> -hexane	6-0.5 <i>n</i> -hexane	7- <i>n</i> -hexane
formula	C ₇₈ H ₉₈ Ge ₂ N ₂	C ₇₈ H ₉₈ N ₂ Sn ₂	C ₆₆ H ₉₀ NSiSn ₂	C ₇₁ H ₉₆ Ge ₂ N
fw	1208.76	1300.96	1162.86	1108.67
color, habit	yellow, prism	dark red, plate	orange, plate	red, needle
cryst syst	orthorhombic	monoclinic	monoclinic	monoclinic
space group	<i>Pna</i> 2 ₁	<i>P</i> 2 ₁	<i>I</i> 2/ <i>a</i>	<i>P</i> 2 ₁ / <i>c</i>
<i>a</i> (Å)	20.743(4)	11.9584(19)	21.694(4)	14.585(3)
<i>b</i> (Å)	12.008(2)	27.587(5)	18.392(4)	18.300(4)
<i>c</i> (Å)	27.095(5)	20.622(3)	32.292(7)	24.129(5)
α (deg)	90	90	90	90
β (deg)	90	90.114(7)	96.47(3)	90.03(3)
γ (deg)	90	90	90	90
<i>V</i> (Å ³)	6749(2)	6803(2)	12803(4)	6440(2)
<i>Z</i>	4	4	8	4
cryst dims, mm	0.40 × 0.28 × 0.28	0.52 × 0.46 × 0.22	0.12 × 0.10 × 0.02	0.34 × 0.34 × 0.12
<i>d</i> _{calc} , g/cm ³	1.190	1.270	1.207	1.143
μ, mm ^{−1}	1.411	0.777	0.835	0.972
no. of reflns	6496	40367	11720	14754
no. of obsd reflns	4765	37791	7157	10483
<i>R</i> , obsd reflns	0.0328	0.0281	0.0577	0.0828
<i>wR</i> ₂ , all	0.0779	0.0631	0.1736	0.1961

compd	8-0.5Et ₂ O 0.65PhCN 0.35Me(<i>c</i> -Pent)	9- <i>n</i> -hexane	10-0.5 <i>n</i> -hexane	11-(Et ₂ O) _{2.25}	14-(Et ₂ O) _{0.5}
formula	C _{83.65} H _{98.45} Ge ₂ N _{2.65}	C ₇₈ H ₁₁₈ Ge ₂ N ₄ Si ₃	C ₆₃ H ₈₃ Ge ₂ O ₅	C ₁₄₇ H _{170.50} Ge ₄ N ₁₂ O _{2.25}	C ₉₆ H ₁₀₄ Ge ₂ O
fw	1286.18	1341.21	1065.47	2431.81	1418.97
color, habit	orange yellow, plate	yellow, plate	colorless, block	pale yellow, block	yellow, rod
cryst syst	triclinic	triclinic	monoclinic	monoclinic	triclinic
space group	<i>P</i> 1̄	<i>P</i> 1̄	<i>P</i> 2 ₁ / <i>c</i>	<i>P</i> 2 ₁ / <i>n</i>	<i>P</i> 1̄
<i>a</i> (Å)	13.0890(17)	12.8515(9)	14.868(6)	19.3869(9)	13.7999(8)
<i>b</i> (Å)	14.2078(17)	14.9117(11)	18.065(7)	29.4879(13)	15.1927(9)
<i>c</i> (Å)	21.234(3)	20.4565(15)	22.078(9)	25.0943(11)	20.3401(12)
α (deg)	93.795(3)	80.746(3)	90	90	87.3680(10)
β (deg)	91.656(3)	80.117(3)	104.633(9)	102.0570(10)	79.4960(10)
γ (deg)	115.630(3)	83.322(4)	90	90	66.6180(10)
<i>V</i> (Å ³)	3545.2(8)	3795.9(5)	5737(4) Å ³	14029.4(11)	3847.0(4)
<i>Z</i>	2	2	4	4	2
cryst dims, mm	0.40 × 0.24 × 0.10	0.30 × 0.23 × 0.15	0.12 × 0.09 × 0.05	0.20 × 0.15 × 0.14	0.46 × 0.19 × 0.15
<i>d</i> _{calc} , g/cm ³	1.205	1.173	1.233	1.151	1.225
μ, mm ^{−1}	0.893	0.882	1.094	0.902	0.830
no. of reflns	21151	17358	7505	24669	17678
no. of obsd reflns	15425	13971	3607	15875	12284
<i>R</i> , obsd reflns	0.0468	0.0356	0.0907	0.0663	0.0425
<i>wR</i> ₂ , all	0.1317	0.0937	0.2620	0.1814	0.1119

overnight to give dark red crystals of **12** (0.15 g, 78%). Mp: 178 °C. ¹H NMR (C₆D₆, 300.08 MHz): δ 0.77 (br, 24H, CHMe₂), 1.07 (br, 24H, CHMe₂), 3.04 (sept, 8H, *J* = 6.6 Hz, CHMe₂), 6.65 (d, 4H, *J* = 2.5 Hz, Ar–H), 6.71 (d, 6H, *J* = 2.5 Hz, Ar–H), 6.98 (d, 6H, *J* = 7.5 Hz, Ar–H), 7.09–7.21 (m, 6H, Ar–H), 7.29 (d, 4H, *J* = 6.9 Hz, Ar–H). ¹³C{¹H} NMR (C₆D₆, 100.52 MHz): δ 23.5 (CHMe₂), 26.1 (CHMe₂), 31.1 (CHMe₂), 123.5, 126.4, 127.1, 129.1, 129.3, 130.8, 138.0, 140.2, 145.7, 146.8, 147.5, 159.2 (unsaturated carbon). UV–vis (hexane): 375 nm (shoulder). The compound was **13** prepared in a manner similar to **12**, after work up yellow crystals of **13** were obtained at −20 °C from *n*-hexane (0.12 g, 84%). Mp: 225 °C (dec). ¹H NMR (C₆D₆, 300.08 MHz): δ −0.21 (s, 9H, SiMe₃), −0.15 (s, 9H, SiMe₃), 0.24 (d, 6H, CHMe₂), 0.90, 1.01, 1.19, 1.23–1.45 (m, 42H, CHMe₂), 1.68 (br, 1H, CHMe₂), 2.03 (sept, 1H, *J* = 6.7 Hz, CHMe₂), 2.28 (sept, 1H, *J* = 6.7 Hz, CHMe₂), 2.82 (sept, 2H, *J* = 6.7 Hz, CHMe₂), 3.05 (sept, 2H, *J* = 6.7 Hz, CHMe₂), 3.35 (sept, 1H, *J* = 6.7 Hz, CHMe₂), 5.38 (br s, 1H, α-CH), 5.76 (br s, 1H, α-CH), 6.58 (d, 2H, *J* = 7.5 Hz, Ar–H), 6.98–7.24 (m, 13H, Ar–H), 7.50 (d, 2H, *J* = 7.4 Hz, Ar–H). ¹³C{¹H} NMR (C₆D₆, 75.5 MHz): δ −1.58 (SiMe₃), −1.28 (SiMe₃), 12.95 (CHMe₂), 17.84 (CHMe₂), 19.64 (CHMe₂), 21.64 (CHMe₂), 24.41 (CHMe₂), 29.71 (CHMe₂), 32.78 (CHMe₂), 34.57 (CHMe₂), 50.05 (α-C), 121.67, 122.74, 124.6, 126.08, 130.46, 131.06, 140.48, 145.14, 147.11, 159.21, 163.55 (unsaturated carbon). The compound **14** was prepared in the same manner as that

described for **12**. The crude product was recrystallized from diethyl ether to give yellow crystals of **14**. ¹H NMR (C₆D₆, 300.08 MHz): δ 0.41, 0.55, 0.72, 0.83, 0.91, 0.96, 1.06, 1.08, 1.13, 1.29, 1.53, 1.92, 1.98, 2.21, 2.49, 2.85, 3.10, 3.22, 3.40, 3.90, 5.66, 5.91, 6.65, 6.84–7.34, 9 (m). ¹³C{¹H} NMR (C₆D₆, 100.52 MHz): δ 15.44, 21.00, 21.30, 21.85, 22.52, 23.06, 23.69, 24.07, 24.20, 24.31, 25.15, 25.24, 25.43, 25.72, 26.52, 27.70, 28.44, 30.05, 30.53, 30.62, 30.72, 31.09, 31.84, 38.48, 50.94, 65.76, 91.71, 93.85, 94.86, 95.07, 120.56, 122.26, 122.73, 123.19, 123.42, 124.23, 124.44, 125.95, 126.09, 126.23, 126.44, 126.50, 127.14, 128.65, 128.98, 129.79, 130.72, 131.34, 131.61, 135.43, 135.70, 137.28, 137.49, 138.58, 140.56, 140.99, 141.65, 144.89, 145.63, 146.18, 146.47, 146.72, 147.10, 147.23, 147.36, 147.42, 149.86, 150.46, 150.61, 166.17, 166.86.

X-ray Crystallographic Studies. The crystals were removed from the Schlenk tube under a rapid flow of argon and immediately submerged in hydrocarbon oil. A suitable crystal was selected, mounted on a glass fiber attached to a copper pin, and rapidly placed in the cold stream of N₂ of the diffractometer for data collection. Data for **3** were collected at 130 K on a Siemens P4 diffractometer with use of Cu Kα (λ = 1.4152 Å) radiation. Data for **4** (93 K), **6** (93 K), **7** (91 K), **8** (93 K), **9** (150 K), and **10** (90 K) were collected on a Bruker SMART 1000, and data for **11** and **14** were collected at 90 K with a Bruker SMART APEX II diffractometer with use of Mo Kα (λ = 0.71073 Å) radiation and a CCD area detector. Empirical absorption

corrections were applied by using SADABS or XABS.¹⁹ The structures were solved with use of either direct methods or the Patterson option in SHELXS and refined by the full-matrix least-squares procedures in SHELXL.²⁰ All non-hydrogen atoms were refined anisotropically while hydrogens were placed at calculated positions and included in the refinement using a riding model. The structures of compound **6**, **7**, and **10** exhibit somewhat poorer C–C bond precision and instances of large thermal motion than the others. For **6** and **10**, these problems arise primarily from small crystal size. In the case of structure **10**, few high angle data were observed, and fewer than 50% of the independent data below $2\theta = 45^\circ$ have $I > 2\sigma(I)$. Structure **7** was refined as a rotational twin, with twin law [1 0 0 0 –1 0 0 0 –1]; twin parameter 0.471(2). Thermal parameters were restrained by use of the SHELXL ISOR 0.008 command; however, some anomalous thermal motion is still evident in the peripheral Pr^i groups. Some details of data collection and refinement are provided in Table 1. Further details are in the Supporting Information.

Results

The reactions undergone by the germanium and tin alkyne analogues **1** and **2** are shown in Scheme 1.

We first examined the reactions of **1** and **2** with azobenzene which yielded the products **3** and **4**. It is probable that the reaction proceeds via a [2 + 2] addition pathway. A cyclic product was not isolated, however (cf. reaction with PhCCPh to afford **12** below).¹⁶ Furthermore, the addition of an excess of the azobenzene did not induce further reaction, which is consistent with the absence of a reactive E–E bond between the heavier atoms in the molecules.

The molecular structures of **3** and **4** are shown in Figure 1 along with selected bond distances and angles. The structures, which are similar to each other, show that cleavage of the Ge–Ge and Sn–Sn bonds in **1** and **2** has been induced to afford products based on a substituted hydrazine in which the nitrogen atoms carry phenyl as well as $\text{Ar}'\text{Ge}$ or $\text{Ar}'\text{Sn}$ substituents. The N–N bond lengths 1.453(5) Å (**3**) and 1.430(3) Å (avg **4**) are consistent with a single bond.²¹ The coordination of the nitrogens is almost planar in each molecule with angular sums at nitrogen ($\Sigma^\circ\text{N}$) of 358.8(1)° (**3**) and 357.5(2)–358.5(2)° (**4**). The Ge–N bond length (1.879(4) Å avg) is within the range found in other germanium(II) amides (1.83–1.89 Å).²² The average Sn–N distance in **4** (2.107(2) Å) is similar to those found in the two coordinated tin species $\text{Sn}\{\text{N}(\text{SiMe}_3)_2\}_2$ (Sn–N = 2.09(1) Å)²³ and $\text{Sn}\{\text{N}(\text{SiMe}_3)_2\}\{\text{C}_6\text{H}_3-2,6-(\text{C}_6\text{H}_2-2,4,6-\text{Pr}^i_3)_2\}$ (Sn–N = 2.094(5) Å).²⁴ The relative orientation of the nitrogen coordination planes in each molecule is indicated by the high torsion angles for the arrays Ge1–N1–N2–Ge2 (59.6°) and Sn1–N1–N2–Sn2 (57.2°).

Addition of an excess of N_3SiMe_3 to **1** and **2** resulted in the formation of the diradicaloid $\text{Ar}'\text{Ge}\{\mu_2\text{-N}(\text{SiMe}_3)\}_2\text{GeAr}'$ (**5**) and the monoimide bridged species $\text{Ar}'\text{Sn}\{\mu_2\text{-N}(\text{SiMe}_3)\}\text{SnAr}'$ (**6**), respectively (Scheme 1). The structure of **5** has been

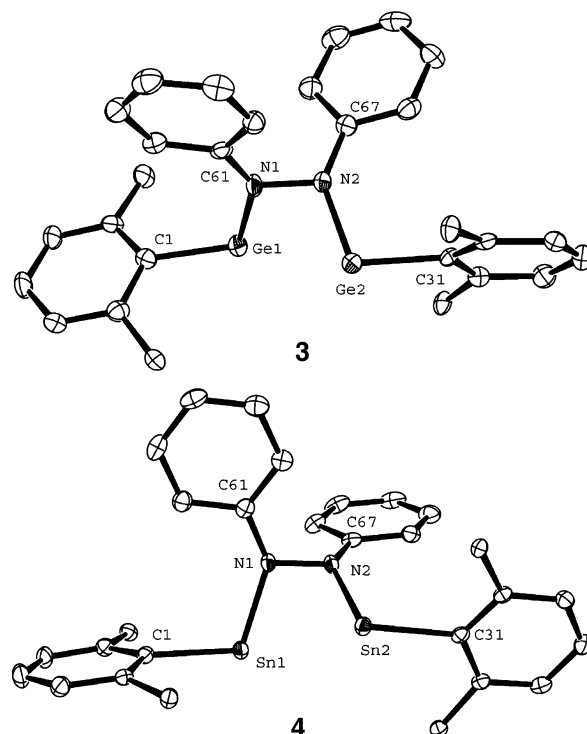


Figure 1. Thermal ellipsoid plots 30% of **3** and **4**. Hydrogen atoms and $\text{C}_6\text{H}_3-2,6-\text{Pr}^i_2$ groups (except ipso carbon atoms) are not shown. Selected bond distances (Å) and angles (deg) for **3**: Ge1–N1 1.882(4), Ge1–C1 2.025(5), Ge2–N2 1.875(4), Ge2–C31 2.039(5), N1–N2 1.453(3); Ge–Ge 3.106(1); N1–Ge1–C1 106.14(18), N2–Ge2–C31 105.06(18), Ge1–N1–N2 106.5, Ge2–N2–N1 107.2(3). For **4**, the asymmetric unit contains two almost identical molecules, one of which is shown: Sn1–N1 2.106(2), Sn1–C1 2.218(3), Sn2–N2 2.109(2), Sn2–C31 2.217(3), N1–N2 1.429(3); Sn1–Sn2 3.2257(6); C1–Sn1–N1 106.44(9), Sn1–N1–N2 105.34(15), N1–N2–Sn2 106.23(15), N2–Sn2–C31 103.65(9).

reported in a previous communication and is illustrated schematically in Scheme 1.¹⁶ It consists of a planar Ge_2N_2 core in which the geometry at nitrogen is also planar while that at germanium is pyramidal, $\Sigma^\circ\text{Ge} = 322.10(7)^\circ$ with the Ar' substituents arranged in a trans fashion across the core. The Ge–N bond lengths, 1.863(2) and 1.874(2) Å, are within the range found in other dimeric ring species (1.70–1.88 Å).²⁵ In sharp contrast, the reaction of **2** with N_3SiMe_3 produced the new imide bridged species **6**. It has the structure illustrated in Figure 2.

It can be seen that a $\text{N}(\text{SiMe}_3)$ unit bridges two $\text{Ar}'\text{Sn}$ moieties. The two Sn–N distances (2.111(6) and 2.055(6) Å) are slightly different and are similar to those found in **4** which is consistent with single bonding. The geometry at the nitrogen atom is almost planar ($\Sigma^\circ\text{N} = 358.3(3)^\circ$). The Sn1–N1–Si1 (115.8(3)°) and Sn2–N1–Si1 (134.6(3)°) angles are very dissimilar, however, and the shorter Sn2–N1 bond is associated with the wider Sn2–N1–Si1 angle. Moreover, the ipso carbon (C31) bonded to Sn(2) lies 0.85 Å from the averaged Si1–N1–Sn1–Sn2 plane, whereas the ipso carbon (C1) lies 1.60 Å from this plane. The Sn–C (aryl) distances are slightly longer than those observed in $\text{Sn}(\text{Mes}^*)_2$ (2.226(7) Å ($\text{Mes}^* = 2,4,6-$

(19) SADABS an empirical absorption correction program from the SAINTPlus NT, version 5.0 package; Bruker AXS: Madison, WI, 1998.

(20) SHELXL, version 5.1; Bruker AXS: Madison, WI, 1998.

(21) The N–N bond length in $(\text{H}_3\text{Si})_2\text{NN}(\text{SiH}_3)_2$ is 1.46(2) Å; Glidewell, C.; Rankin, D. W. H.; Robiette, A. G.; Sheldrick, G. M. *J. Chem. Soc. A.* **1970**, 318.

(22) See for example: (a) Schaefer, A.; Saak, W.; Weidenbruch, M. *Z. Anorg. Allg. Chem.* **1998**, 624, 1405. (b) Veith, M.; Rammo, A. *Z. Anorg. Allg. Chem.* **2001**, 627, 662.

(23) Fjeldberg, T.; Hope, H.; Lappert, M. F.; Power, P. P.; Thorne, A. J. *Chem. Commun.* **1983**, 639.

(24) Pu, L.; Olmstead, M. M.; Power, P. P.; Schiemenz, B. *Organometallics* **1998**, 17, 5602.

(25) Hitchcock, P. B.; Lappert, M. F.; Thorne, A. J. *Chem. Commun.* **1990**, 1587. Ahlemann, J. T.; Roesky, H. W.; Murugavel, R.; Parsini, E.; Noltemeyer, M.; Schmidt, H. G.; Müller, O.; Herbst-Irmer, R.; Markovskii, L. N.; Shermolovich, Y. G. *Chem. Ber.* **1997**, 130, 1133. Bartlett, R. A.; Power, P. P. *J. Am. Chem. Soc.* **1990**, 112, 3660.

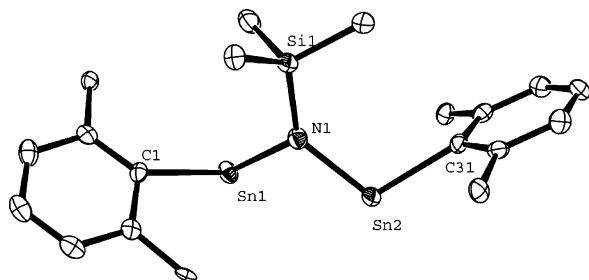


Figure 2. Thermal ellipsoid plot (30%) of **6**. Hydrogen atoms and $\text{C}_6\text{H}_3\text{-2,6-Pr}_2$ groups (except ipso carbon atoms) are not shown. Selected bond distances (Å) and angles (deg): Sn1–N1 2.111(6), Sn1–C1 2.267(7), Sn2–N1 2.055(6), Sn2–C31 2.250(7), N1–Si1 1.732(6); N1–Sn1–C1 107.0(2), N1–Sn2–C31 108.1(2), Sn1–N1–Sn2 107.9, Sn1–N1–Si1 115.8(3), Sn2–N1–Si1 134.6(3).

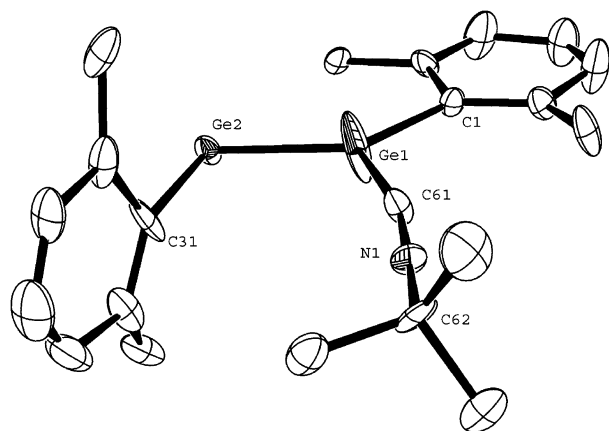


Figure 3. Thermal ellipsoid plot of **7**. Hydrogen atoms and $\text{C}_6\text{H}_3\text{-2,6-Pr}_2$ groups (except ipso carbon atoms) are not shown. Selected bond distances (Å) and angles (deg): Ge1–Ge2 2.3432(9), Ge1–C1 1.966(5), Ge1–C61 1.957(5), C61–N1 1.155(2), N1–C62 1.480(6), Ge2–C31 2.004(5); Ge2–Ge1–C1 129.62(14), Ge1–Ge2–C31 102.77(15), Ge2–Ge1–C61 127.61(2), C1–Ge1–C61 112.7(2), Ge1–C61–N1 164.2(6), C61–N1–C62 168.3(11).

$\text{Bu}'_3\text{C}_6\text{H}_2$),²⁶ $\text{Sn}\{\text{N}(\text{SiMe}_3)_2\}\{\text{C}_6\text{H}_3\text{-2,6}(\text{C}_6\text{H}_2\text{-2,4,6-Pr}'_3)_2\}$ (2.225(5) Å),²⁴ and $\{\text{Ar}'\text{Sn}(\mu_2\text{-Cl})\}_2$ (2.225(6) Å).^{14,27}

The “digermine” **1** reacted smoothly with *t*-BuNC, PhCN, and $\text{N}_2\text{CHSiMe}_3$ at ca. 25 °C to afford respectively the dark red 1:1 isonitrile adduct **7** (Scheme 1), the cyclic product **8** which features a $\text{C}_2\text{N}_2\text{Ge}_2$ six-membered ring, and the unusual triply bridged species **9**. In contrast, the tin analogue **2** reacts with neither $\text{Bu}'\text{NC}$ nor PhCN under the same conditions as those for **2**. It reacts slowly with $\text{N}_2\text{CHSiMe}_3$, but this leads to complicated mixtures as indicated by the ^1H NMR spectrum. We have been unable to isolate any pure product from the reaction under various conditions that involved different ratios of **2** and $\text{N}_2\text{CHSiMe}_3$.

The X-ray structure of **7** (Figure 3) shows that the *tert*-butyl isonitrile molecule is coordinated through carbon to one of the germanium atoms. The coordination of the isonitrile occurs in the molecular plane formed by the C1,Ge1,Ge2,C31 core of $\text{Ar}'\text{GeGeAr}'$ to afford an almost planar C31,Ge2,Ge1,C1,C61 array. The geometry at the isonitrile carbon C61 deviates somewhat from linearity (Ge1–C61–N1 = 164.2(6)°, and the C61–N1 distance, 1.155(20) Å, indicates that the CN triple bond

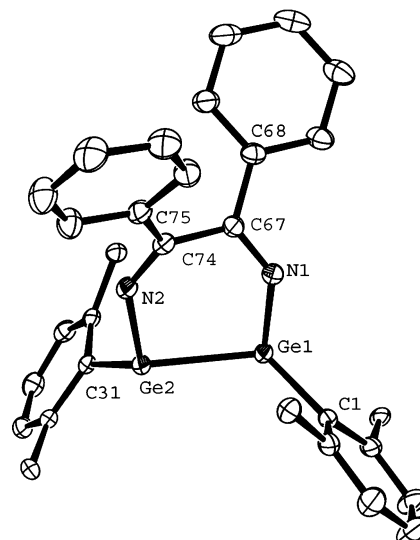


Figure 4. Thermal ellipsoid plot (30%) of **8**. Hydrogen atoms and $\text{C}_6\text{H}_3\text{-2,6-Pr}_2$ rings (except ipso carbon atoms) are not shown. Selected bond distances (Å) and angles (deg): Ge1–N1 1.8060(18), Ge1–Ge2 2.4963(4), Ge2–N2 1.8009(18), N2–C74 1.281(3), C74–C67 1.517(3), C67–N1 1.280(3), Ge1–C1 1.982(2), Ge2–C31 1.980(2); N1–Ge1–Ge2 96.33(6), N1–Ge1–C1 108.39(8), C1–Ge1–Ge2 120.92(6), Ge1–Ge2–N2 96.94(6), Ge1–Ge2–C31 119.68(6), N2–Ge2–C31 109.21(8), Ge1–N1–C67 137.08(16), N1–C67–C74 119.28(19), C67–C74–N2 119.58(19), C74–N2–Ge2 136.35(15).

is retained in the reaction. The three-coordinate Ge1 atom has a planar geometry ($\Sigma^\circ\text{Ge} = 360.0(2)^\circ$), and the Ge2–Ge1–C1 bond angle (129.62(14)°) is very close to that found in the parent digermine $\text{Ar}'\text{GeGeAr}'$ (128.67(8)°).⁹ In contrast, the Ge1–Ge2–C31 angle (102.77(15)°) at the base-free Ge2 is 25.9° narrower than that in the digermine $\text{Ar}'\text{GeGeAr}'$ suggesting the lone pair at the Ge2 atom is now much more localized. The Ge1–Ge2 distance (2.3432(9) Å) is 0.058 Å longer than that in the $\text{Ar}'\text{GeGeAr}'$ precursor (2.285(5) Å) but remains considerably shorter than a normal Ge–Ge single bond (ca. 2.44 Å), indicating the retention of significant multiple-bonding character. The Ge–Ge distance in **7** resembles that in the digermene, $\text{Ar}^*(\text{Me})\text{GeGe}(\text{Me})\text{Ar}^*$ ($\text{Ar}^* = \text{C}_6\text{H}_3\text{-2,6}(\text{C}_6\text{H}_2\text{-2,4,6-Pr}'_3)_2$; Ge–Ge = 2.3173(3) Å).²⁷ The Ge1–C1 distance is marginally shorter (by 0.038 Å) than that of Ge2–C31 even though the coordination number at Ge1 is higher (3 versus 2) than that of the Ge2 atom. The Ge1–C61 donor–acceptor bond length (1.957(5) Å) is slightly shorter than those of both Ge–C sigma bonds and indicates very strong electron donation by the isonitrile to the germanium atom.

Upon reaction of **1** with PhCN, compound **8** (Figure 4), which has a unique quasi-aromatic six-membered ring, is formed. The compound is effectively a pyrazine analogue which has incorporated two germanium atoms instead of carbons in its ring. The ring is rather distorted from planarity, and the average deviations (Å) of the ring atoms from the least squares plane are N1(−0.054), Ge1(−0.053), Ge2(+0.05), N2(+0.060), C67(+0.20), and C74(+0.204). The geometry at each germanium is quite pyramidal ($\Sigma^\circ\text{Ge1} = 325.64(7)^\circ$, $\Sigma^\circ\text{Ge2} = 325.83(7)^\circ$, respectively). Moreover, the Ge1–Ge2 bond length (2.4963(4) Å) is slightly longer than the Ge–Ge single bond length (2.44 Å) in elemental germanium.^{29a} The Ge–N bond lengths (average 1.803(3) Å) correspond to a single bond. The N1–C67 (1.280-

(26) Weidenbruch, M.; Schlaefke, J.; Schäfer, A.; Peters, K.; von Schnering, H. G.; Marsmann, H. *Angew. Chem., Int. Ed.* **1994**, *33*, 1846.

(27) Eichler, B. E.; Pu, L.; Stender, M.; Power, P. P. *Polyhedron* **2001**, *20*, 551.

(28) Stender, M.; Pu, L.; Power, P. P. *Organometallics* **2001**, *20*, 1820.

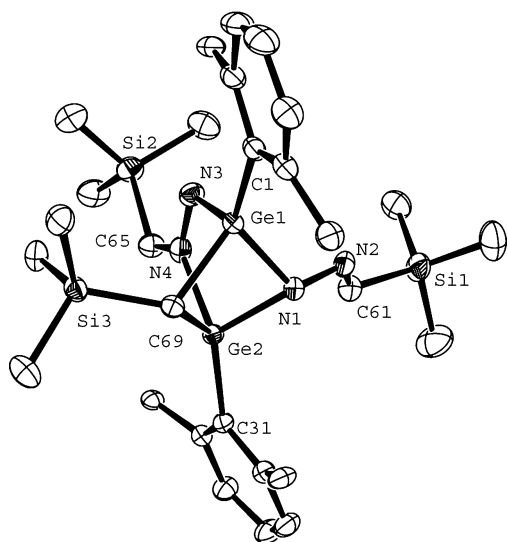


Figure 5. Thermal ellipsoid plot (30%) of **9**. Hydrogen atoms and $\text{C}_6\text{H}_3\text{-2,6-Pr}_2$ rings (except ipso carbon atoms) are not shown. Selected bond distances (Å) and angles (deg): Ge1–N1 1.9191(16), Ge1–N3 1.8749(17), Ge1–C1 1.9722(19), Ge1–C69 2.0022(18), Ge2–N1 1.9231(16), Ge2–N4 2.0437(16), Ge2–C69 1.9720(18), Ge2–C31 1.9943(18); N1–N2 1.394(2), N3–N4 1.341(2), N2–C61 1.274(3), N4–C65 1.314(3); N1–Ge1–C1 128.55(7), N1–Ge1–N3 97.78(7), N1–Ge1–C69 84.29(7), C1–Ge1–N3 116.88(8), C1–Ge1–C69 123.13(7), N3–Ge1–C69 98.34(8), N1–Ge2–N4 90.80(7), N1–Ge2–C31 118.18(7), N1–Ge2–C69 85.01(7), N4–Ge2–C31 127.05(7), N4–Ge2–C69 91.29(7), C31–Ge2–C69 131.50(8), Ge1–N1–N2 118.10(12), Ge1–N1–Ge2 85.87(6), Ge2–N1–N2 126.73(13), Ge1–N3–N4 106.13(12), Ge2–N4–N3 111.61(12), N3–N4–C65 120.43(17), Ge2–N4–C65 127.94(15), Ge1–C69–Ge2 82.37(7), Ge1–C69–Si3 116.38(10), Ge2–C69–Si3 124.22(10).

(3) Å) and N2–C74 (1.281(3) Å) bond lengths are consistent with C=N double bonding,^{29b} and the C67–C74 bond (1.517(3) Å) is obviously a single one.

The structure of **9** is shown in Figure 5. The most interesting feature of this compound is that it possesses three different types of bridging units that result from the reaction of **1** with trimethylsilyldiazomethane. One molecule of $\text{N}_2\text{CH}(\text{SiMe}_3)$ eliminates N_2 to form an alkylidene moiety that bridges two germaniums. Two $\text{N}_2\text{CHSiMe}_3$ molecules are found to bridge the two germaniums through the NN moiety in one case and through the terminal N atom in the other. The germaniums are four coordinate and have distorted tetrahedral geometry which shows that the original Ge–Ge bond in **1** has been destroyed. The bridging Ge–C(69) bond lengths indicate normal Ge–C single bonds.^{29a} The Ge1–N1 (1.919(2) Å) and Ge2–N1 (1.923(2) Å) bond lengths involving the $\mu_2:\eta^1$ bridging $\text{N}_2\text{CH}(\text{SiMe}_3)$ ligand are slightly longer than those found in compounds **3** (avg 1.879(4) Å) and **5** (avg 1.868(6) Å). However, the bridging distances involving the $\mu_2:\eta^2\text{-N}_2\text{CH}(\text{SiMe}_3)$ moiety Ge1–N3 (1.875(2) Å) and Ge2–N4 (2.044(2) Å) differ considerably, possibly as a result of the greater coordination number of N4 in comparison to N3. The N1–N2 (1.394(2) Å) and N3–N4 (1.341(2) Å) distances indicate retention of multiple N–N bond character.^{29b} The geometry of the N1 atom is pyramidal ($\Sigma^\circ\text{N1} = 330.70(10)^\circ$), whereas the N4 atom has a planar geometry ($\Sigma^\circ\text{N4} = 359.98(15)^\circ$).

When **1** was exposed to an excess of N_2O at normal pressure, its red color disappeared immediately to give a pale yellow

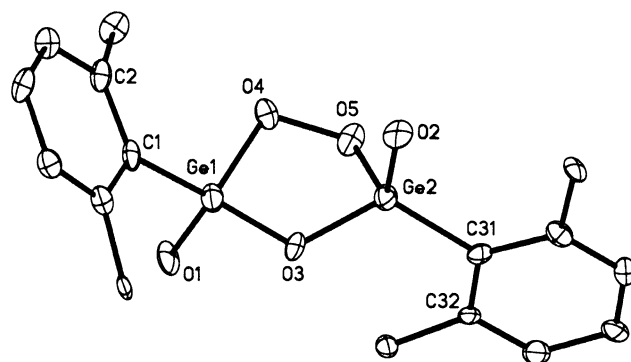
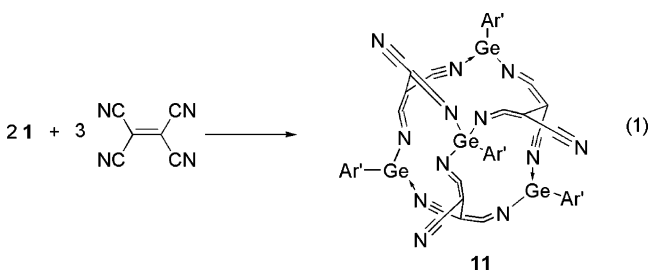


Figure 6. Thermal ellipsoid plot (30%) of **10**. Hydrogen atoms and $\text{C}_6\text{H}_3\text{-2,6-Pr}_2$ rings (except ipso carbon atoms) are not shown. Selected bond distances (Å) and angles (deg): Ge1–O1 1.759(7), Ge1–O3 1.754(7), Ge1–O4 1.822(7), Ge1–C1 1.925(11), Ge2–O2 1.755(7), Ge2–O3 1.750(7), Ge2–O5 1.836(8), Ge2–C31 1.932(11), O4–O5 1.501(10), Ge1–Ge2 2.885(2), Ge1–O3–Ge2 110.8(4), Ge1–O4–O5 109.5(5), Ge2–O5–O4 104.8(5), O3–Ge1–O4 110.3(4), O3–Ge2–O5 110.7(4).

solution within five minutes. The germanium peroxide product $\text{Ar}'(\text{OH})(\mu_2\text{-O})\text{Ge}(\mu_2:\eta^2\text{-O}_2)\text{Ge}(\text{OH})\text{Ar}'$ (**10**) was obtained after standard workup. Single-crystal X-ray analysis afforded the structure shown in Figure 6.

It consists of a core Ge_2O_5 puckered ring in which the germaniums are linked by oxo and peroxo bridges. The germaniums are each bound to a terminal hydroxo and Ar' group disposed in a trans fashion with respect to each other across the ring. The Ge–O bonds to the hydroxo and μ -oxo moieties are similar (1.755(8) Å avg) but shorter than the Ge–O distances to the peroxide oxygens (1.829(8) Å avg). The former values resemble the average distance (1.78(4) Å) observed in more than 400 structures which feature a $\text{Ge}(\mu\text{-O})\text{Ge}$ unit.³⁰ The latter is consistent with the average distance (1.81(4) Å) in the three known complexes in which two germaniums are bridged by peroxide.³¹ The O–O bond length 1.50(1) Å is slightly longer than the mean O–O bond length 1.45(2) Å observed in these complexes. It is possible that the reaction proceeds through a radical mechanism to form $\text{Ar}'\text{GeOOGeAr}'$ units, which react with further equivalents of N_2O with subsequent hydrogen atom abstraction from the solvent to give the peroxy and oxy bridges and the terminal hydroxy groups, respectively.

Compound **1** reacts with tetracyanoethylene in ether to give the unexpected compound **11** as shown schematically in eq 1. The reaction involves the reduction of six cyano groups from three molecules of tetracyanoethylene to form a large fused ring system **11** in which Ge(1) is polar covalently bound to three cyano nitrogens each from separate TCNE moieties. A different



(29) (a) Wells, A. F. *Structural Inorganic Chemistry*, 5th ed.; Clarendon: Oxford, 1984; p 1173. (b) Wells, A. F. *Structural Inorganic Chemistry*, 5th ed.; Clarendon: Oxford, 1984; p 807.

(30) Cambridge Crystallographic Data Center, Cambridge, UK, 2001.

(31) (a) Masamune, S.; Batcheller, S. A.; Park, J.; Davis, W. M.; Yamashita, O.; Ohta, Y.; Kabe, Y. *J. Am. Chem. Soc.* **1989**, *111*, 1888. (b) Kako, M.; Akasaka, T.; Ando, W. *Chem. Commun.* **1992**, 457.

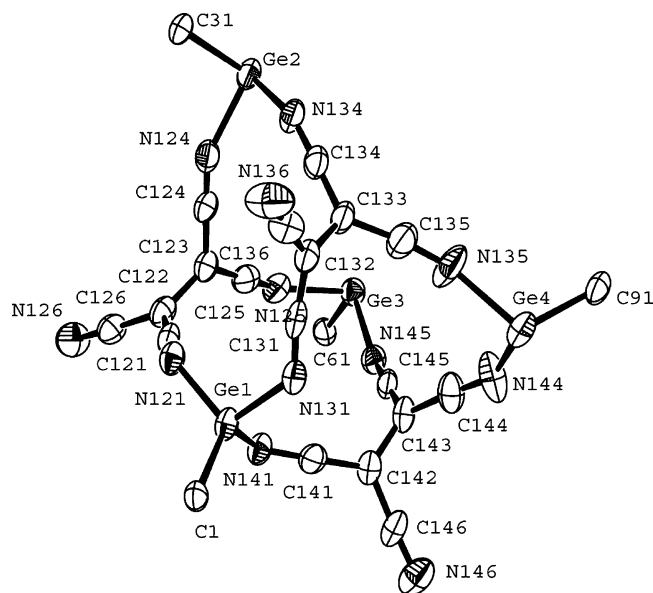


Figure 7. Thermal ellipsoid plot (30%) of **11**. Hydrogen atoms and Ar' rings (except ipso carbon atoms) are not shown. Selected bond distances (Å) and angles (deg): Ge1–C1 1.917(4), Ge1–N121 1.853(4), Ge1–N131 1.847(4), Ge1–N141 1.859(4), Ge2–C31 2.013(5), Ge2–N124 2.027(4), Ge2–N134 2.023(4), Ge3–C61 2.008(5), Ge3–N125 2.025(4), Ge3–N145 2.027, Ge4–C91 1.942(6), Ge4–N135 2.040(5), Ge4–N144 2.012(5), N121–C121 1.202(6), C121–C122 1.354(7), C122–C123 1.466(7), C123–C124 1.371(7), C124–N124 1.156(6), N134–C134 1.164(6), C134–C133 1.379(7), C133–C135 1.375(6), C135–N135 1.148(6), N144–C144 1.160(6), C144–C143 1.361(7), C143–C142 1.486(7), C142–C141 1.323(6), C141–N141 1.205(5), N131–Ge1–N121 100.64(16), N131–Ge1–N141 102.41(16), N121–Ge1–N141 102.59, N131–Ge1–C1 114.89(17), N121–Ge1–C1 121.15(17), N141–Ge1–C1 112.72, C31–Ge2–N134 96.80(17), C31–Ge2–N124 99.95(17), N134–Ge2–N124 86.57(16), C61–Ge3–N125 96.88(17), C61–Ge3–N145 101.43(17), N125–Ge3–N145 86.80(15), C91–Ge4–N144 95.3(2), C91–Ge4–N135 103.0(3), N144–Ge4–N135 87.2(3).

nitrogen from each TCNE is bound to a separate GeAr' moiety, and each of these GeAr' units also behaves as an acceptor of lone pair pair density from a nitrogen from a neighboring TCNE unit. In this way, the fused ring structure in Figure 7 is generated. The formal charges within the compound may be designated by the formula $\text{Ar}'\text{Ge}^{3+}\{(\text{TCNE})^{2-}\}_3\{(\text{GeAr}')^+\}_3$.

The structure of **11** is an unusual example of a large cage system incorporating heavier group 14 elements. There are four large fused rings, the largest of which is an 18-membered ring formed by three germaniums (Ge2, Ge3, and Ge4), six nitrogens, and nine carbon atoms. There are three 14-membered rings that incorporate two germanium, four nitrogen, and eight carbon atoms. Each 14-membered ring shares the four-coordinated, tetravalent bridgehead Ge1 atom which is bonded to an Ar' ligand and three imine nitrogen atoms. In the 18-membered ring, the germanium atoms Ge2, Ge3, and Ge4 are three-coordinate and linked by $-\text{N}=\text{C}=\text{C}-\text{C}\equiv\text{N}$ moieties. These germanium atoms are divalent and have one Ge–C (Ar') and one Ge–N sigma bond, with the other coordination site being occupied by a Ge–N dative bond from a nitrile moiety.

The reaction of **1** with PhCCPh and HCCSiMe₃ has been previously communicated by us.¹⁶ The reactions give either a stable Ge–C–C–Ge four-membered 1,2-digermacyclobutadiene ring **12** (with PhCCPh) or further reaction (in the case of HCCSiMe₃) to give the intermediate **II** which activates a C=C bond in one of the flanking Dipp rings to give **13**. We proposed that the intermediate **II** has 1,4-diradical character (eq 2) which

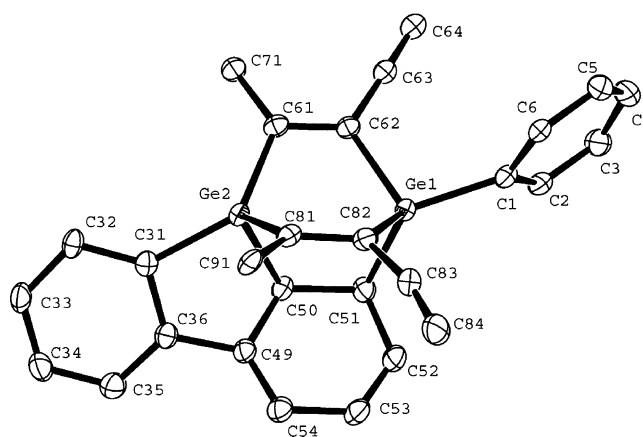
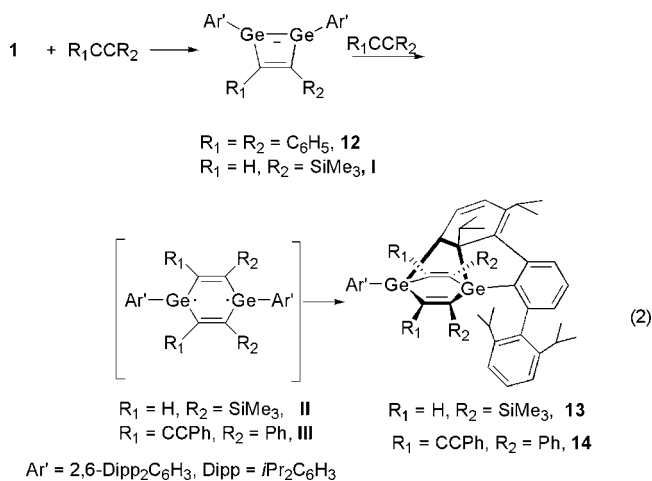


Figure 8. Thermal ellipsoid plot (50%) of **14**. Hydrogen atoms and Dipp and phenyl rings (except the Dipp ring involved in the addition reaction) are not shown. Selected bond distances (Å) and angles (deg): Ge1–C1 1.981(2), Ge1–C51 2.021(2), Ge1–C62 1.996(2), Ge1–C82 1.956(2), Ge2–C31 1.947(2), Ge2–C50 2.023(2), Ge2–C61 1.945(2), Ge2–C81 1.978(2), C49–C50 1.529(3), C50–C51 1.563(3), C51–C52 1.482(3), C52–C53 1.326(3), C53–C54 1.452(3), C54–C49 1.355(3), C61–C62 1.364(3), C81–C82 1.361(3), Ge1–Ge2 3.089, C1–Ge1–C51 125.38(9), C1–Ge1–C62 104.29(9), C1–Ge1–C82 118.49(10), C51–Ge1–C82 97.25(10), C51–Ge1–C62 102.91(9), C61–Ge2–C31 134.64(9), C61–Ge2–C81 108.28(9), C31–Ge2–C81 110.50(9), C61–Ge2–C50 104.47, C31–Ge2–C50 90.11(9), C81–Ge2–C50 101.39(9).

could be responsible for the activation of the C=C bond in the flanking C₆H₃-2,6-Pr₂ ring. To isolate the intermediate and



obtain further evidence to support this mechanism, we employed the diacetylene PhC≡C–C≡CPh for the reaction. **1** takes up 2 equiv of PhC≡C–C≡CPh at room temperature and reacts with one of the triple bonds in the PhC≡C–C≡CPh molecule in a manner similar to Me₃SiCCH followed by activation of one of the C₆H₃-2,6-Pr₂ rings in Ar'. The regioselectivity of this reaction is the same as that observed in the reaction with HCCSiMe₃ and only isomer **14** was isolated.

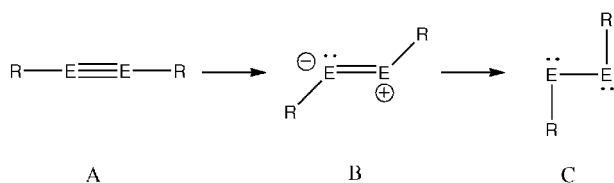
The molecular structure of compound **14** is shown in Figure 8 along with selected bond distances and angles. The germanium atoms have a distorted tetrahedral geometry and are connected by three C–C units to form three six-membered rings. The C50–C51 distance (1.563(3) Å) corresponds to a C–C single bond. The Ge1–C51 and Ge2–C50 bond lengths (2.021(2) and 2.027(2) Å) are longer than those of the other Ge1–C bonds because of the sp³ hybridized C51 atom.

Unlike **1**, **2** did not react with the acetylenes PhCCCPH, HCCSiMe₃, or PhCCCCPh under the same conditions.

Discussion

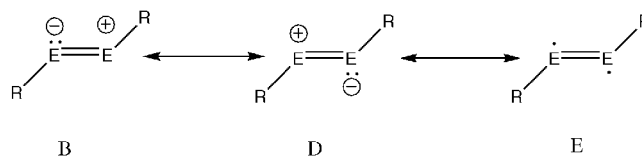
With the exception of the previously reported reaction of Ar*GeGeAr* (Ar* = C₆H₃-2,6(C₆H₂-2,4,6-Prⁱ₃)₂) with 2,3-dimethyl-1,3-butadiene, which afforded Ar*Ge(CH₂C(Me)C(Me)CH₂)CH₂C(Me)=] ¹³, the reactions undergone by Ar*EEAr' (E = Ge or Sn), as depicted in Scheme 1, represent the first experimental studies of the reactivity of heavier group 14 element alkyne analogues with unsaturated molecules. The reactions demonstrate the highly reactive nature of the Ge—Ge multiple bond and the significantly lower reactivity of the corresponding tin—tin interaction. The lower reactivity of the tin species is counterintuitive on the basis of bond strengths (Sn—Sn bonds are weaker than Ge—Ge bonds), steric factors (tin is larger than germanium and is thus less protected by the same ligand), and the greater polarity of the Sn—C bond versus the Ge—C bond. Possible reasons for the greater reactivity of the germanium species are discussed below.

The EE Bond. Previous studies have established the planar trans-bent geometry of both **1** (Ge—Ge = 2.285(5) Å; Ge—Ge—C = 128.67(8)°)⁹ and **2** (Sn—Sn = 2.675(4) Å; Sn—Sn—C = 125.24(7)°)¹⁰ as well as of the lead derivative Ar*PbPbAr* which has a long Pb—Pb bond length of 3.1881(1) Å and a Pb—Pb—C bending angle of 94.26(4)°.⁸ Recent work by Sekiguchi and co-workers has disclosed the preparation and structure of the related silicon species R'SiSiR' (R' = SiPrⁱ{CH(SiMe₃)₂}₂) which also possesses a planar, trans-bent structure with Si—Si = 2.0622(9) Å and a bending angle of 137.44(4)°.¹¹ Thus, stable homonuclear alkyne analogues of all the heavier group 14 elements have now been isolated and characterized. The strong trans-bending observed in all these compounds shows that the bond order is less than three and that nonbonding lone pair character accumulates to an increasing degree at the group 14 element as the group is descended. The bending is thought to be the result of the mixing of an in-plane π-orbital with a σ* orbital whose energies are close enough to cause the interaction of these orbitals in the heavier elements.^{7,12a} The progressive lowering of the bond order may also be represented crudely by the sequence



where A corresponds to a triple bond in acetylene and its derivatives and C represents the bonding in Ar*PbPbAr* in which the Pb—Pb bond is essentially a single one and there is a lone pair at each lead.^{8,32} The bonding is less clearly defined for the Si, Ge, and Sn derivatives. However, it is believed that the bonding in the germanium species is close to that represented by B or D.³³ In valence bond terms, there is an approximate

Ge—Ge double bond and there is a single lone pair that resonates between positions at each germanium as shown by B and D.



It is also possible to represent the structure as the singlet diradical form E³⁴ and this form is supported by calculations.³⁵ The representation of the structure of **1** by the forms B, D, or E suggests high reactivity. For example, in B and D the Ge—Ge bond is depicted as dipolar, and it is a dipole that includes a cationic Ge center that is two-coordinate. These attributes are a prescription for high reactivity as is the singlet diradical form represented by E which often (but not always)³⁶ implies the existence of a relatively low-lying triplet state.

Previously available experimental data and theoretical analysis of molecular energy levels¹³ generally support the applicability of the simple bonding pictures illustrated by forms B–E. For instance, forms B and D suggest that they should be reduced readily. Cyclic voltammetry for **1** has shown that it has a quasi-reversible reduction near 1.38 V vs SCE in THF. Moreover, singly or doubly reduced salts of Ar'GeGeAr' and the related Ar*GeGeAr* (Ar* = C₆H₃-2,6(C₆H₂-2,4,6-Prⁱ₃)₂) can be readily isolated and structurally characterized.^{14,15b} Addition of one electron results in only a small increase (0.048 Å) in the Ge—Ge bond distance to 2.3331(4) Å and a narrowing of the Ge—Ge—C bending angle from 128.67(8)° to 115.55(5)°.¹⁴ This is consistent with the addition of the electron to an essentially nonbonding orbital. Calculations on the MeGeGeMe model species show that the LUMO is the nonbonding n₊ or LP* combination (using MO phraseology).^{33,35} Accordingly, the addition of an electron to this orbital should result in a narrowing of the Ge—Ge—C angle and a slight lengthening of the Ge—Ge bond due to an increase in interelectronic repulsion. This is what is found experimentally.¹⁴ For the tin compound, calculations on the model species MeSnSnMe,³⁵ when its geometry is restricted to that experimentally measured for Ar'SnSnAr', show that like its germanium counterpart the LUMO is the nonbonding n₊, LP* orbital. However, the addition of an electron to Ar'SnSnAr' in THF to give [Ar'SnSnAr'][−] results in a significantly greater lengthening of the SnSn bond from 2.6675(4) to 2.8081(9) Å.¹⁴ Furthermore, the reduction is accompanied by a very large (>27°) decrease in the Sn—Sn—C bond angle from 125.24(7)° to 97.9(2)°.¹⁴ This unexpected behavior can be explained by assuming that in solution the Ar'SnSnAr' has a structure which is more trans-bent than that experimentally observed¹⁰ in the solid state. This assumption is based on calculations³⁵ on the MeSnSnMe model species which show that its lowest energy structure features a more strongly bent Sn—Sn—C angle of 100.0° and a much longer Sn—Sn distance of 3.06 Å (due to the increased 5p character of the orbitals comprising the Sn—Sn σ-bond) than those observed experimentally (2.675(4) Å and 125.24(7)°) for Ar'SnSnAr'. In the more bent, lower energy configuration, the tins possess more

(32) Chen, Y.; Hartmann, M.; Diedenhofen, M.; Frenking, G. *Angew. Chem., Int. Ed.* **2001**, *40*, 2052.

(33) Allen, T. L.; Fink, W. H.; Power, P. P. *Dalton Trans.* **2000**, 407.

(34) Malcolm, N. O. J.; Gillespie, R. J.; Popelier, P. L. A. *Dalton Trans.* **2002**, 3333.

(35) Jung, Y.; Brynda, M.; Power, P. P.; Head-Gordon, M., submitted.

(36) Jung, Y.; Head-Gordon, M. *ChemPhysChem.* **2003**, *4*, 522.

substantial lone pair character and the LUMO is an unfilled π -orbital. In effect, the structure of the neutral $\text{Ar}'\text{SnSnAr}'$ in solution resembles C (like the lead species $\text{Ar}'\text{PbPbAr}'$)⁸ rather than B or D (like its germanium counterpart $\text{Ar}'\text{GeGeAr}'$).⁹ The apparent readiness with which the geometry of the tin species can be changed is consistent with the previous work of Nagase and co-workers³⁷ which showed that such a process requires little energy (see also ref 35). The changed structure of $\text{Ar}'\text{SnSnAr}'$ in solution is also consistent with the fact that it is more readily reduced (-1.21V vs SCE in THF)¹⁴ than its germanium counterpart, since the added electron enters what is, in effect, a π -bonding orbital. The small energy differences between the various geometric configurations in RSnSnR compounds illustrate the finely balanced π -bonding and lone pair tendency of the s-valence electrons.^{35,37,38}

Reactivity of 1 and 2. The different electronic structures of **1** and **2**, as indicated by the changes they undergo upon reduction, are in harmony with the different chemical reactivities shown by **1** and **2**. It can be seen in Scheme 1 that **1** reacts at room temperature with $\text{PhC}\equiv\text{CPh}$, $\text{Me}_3\text{SiC}\equiv\text{CH}$, $:\text{C}\equiv\text{NBU}'$, or $\text{PhC}\equiv\text{N}$, whereas its tin analogue **2** remains unaffected. When **1** or **2** are reacted with N_3SiMe_3 two different products, **5** and **6**, are obtained. The lower reactivity of the tin compound **2** is reflected in the fact that, unlike **1**, it does not react with a second equivalent of N_3SiMe_3 . Instead, the product **6**, which features one NSiMe_3 group bridging two SnAr' fragments, was isolated. The reaction of **1** with $\text{N}_2\text{CH}(\text{SiMe}_3)$ afforded the unusual triply bridged product **9**, and although **2** also reacts slowly with $\text{N}_2\text{CH}(\text{SiMe}_3)$, the products of the reaction are currently unknown. Similarly, **1** reacts with N_2O to produce the unusual peroxo ring species **10**. Compound **2** also reacts with N_2O , but in this case, the products appear to be mixtures of $[\text{Ar}'\text{Sn}(\mu\text{-OH})_2]$ and $[\text{Ar}'\text{Sn}(\mu\text{-O})_2]$ to which no further addition of oxygen occurs.³⁹ The absence of further reaction with oxygen is another manifestation of the lower reactivity of **2**. With TCNE, **1** afforded the unusual fused ring product **11** whereas a similar reaction with **2** has not afforded a crystalline product to date. In summary, for the dozen or so reactions studied so far, the lower reactivity of **2** is reflected in the fact that it either does not react with the unsaturated substrates or it reacts more slowly with them than **1**.

Another notable feature of the reactions described in Scheme 1 is that they result in either complete cleavage of the EE bond or a weakening of the bond to the extent that it is weaker than a single bond. For example, both **1** and **2** react with the unsaturated nitrogen species $\text{PhN}=\text{NPh}$ to give the products **3** and **4** which are isostructural. There are no Ge—Ge or Sn—Sn bonds in these products even though a cyclic Ge_2N_2 species is sterically feasible (cf. cyclic structure of **12** below). It seems likely that the more electronegative nitrogen substituents increase the HOMO—LUMO energy separation which weakens possible MM interactions between the divalent group 14 centers so that no bonding is seen.⁴⁰ No Ge—Ge or Sn—Sn bonding is observed in the products **5**, **6**, **9–11**, **13**, and **14**. A Ge—Ge bond is

apparently retained during the reactions of **1** with $\text{PhC}\equiv\text{N}$ or $\text{PhC}\equiv\text{CPh}$ which give the cyclized derivatives **8** and **12**. However, in these products, the Ge—Ge bonds, which form part of four- and six-membered rings, are quite weak since they have distances of 2.4708(9) and 2.4963(4) Å respectively which are longer than the Ge—Ge distance (2.44 Å) in elemental Ge.^{29a} Furthermore, the germaniums have trigonal pyramidal coordination with interligand angular sums of 325.64(8)° and 325.83-(8)° in **8** and of 318.0(2)° and 317.3(2)° in **12**. In an idealized sense, the cyclizations transform the Ge—Ge “triple” bond in **1** to a “double” bond in **8** and **12**. In reality, however, the structural data show that the transformation involves the conversion of an approximate double bond in **1** to a weakened single bond in **8** and **12**. The Ge—Ge bond orders of less than one in **8** and **12** are also underscored by the pyramidal germanium geometries. The lack of both planarity and significant delocalization in the formally aromatic $\text{C}_2\text{Ge}_2\text{N}_2$ ring in **8** is also notable. The Ge—Ge bond remains essentially undisrupted only in the case of simple 1:1 isonitrile adduct **7**.

Evidence for the Ionic and Diradical Resonance Structures. The structure of the isonitrile adduct **7** shows that the isonitrile coordinates to germanium in the plane formed by the core of the molecule. This is consistent with the n_+ or LP^* character of the LUMO of **1**. Furthermore, the Ge—Ge bond undergoes moderate lengthening which is also in agreement with the generally nonbonding character of the LUMO and with the increase in coordination number at Ge(1). It is notable that the Ge(1)—C(61) distance to the isonitrile carbon is essentially the same as that to the ipso carbon (Ge(1)—C(1)) of the terphenyl ligand. This strong binding of the isonitrile suggests that the germanium is very electrophilic. However, it is the structural changes that occur at the uncomplexed Ge(2) in the $\text{Ar}'\text{GeGeAr}'$ unit that offer deeper insight on the character of the GeGe bond in **1**. Most importantly, the bending angle at Ge(2) is narrowed by over 25° in comparison to that in the precursor: 102.77-(15)° in **7** versus 128.67(8)° in **1**. Moreover, the Ge(2)—C(ipso) bond length increases from 1.996(3) in **1** to 2.004(6) Å in **7**. These changes are consistent with a concentration of the lone pair character at Ge(2) which produces the decrease in the bending angle because of greater lone pair—bond pair repulsion. In effect, the coordination of the isonitrile to **1** “freezes out” one of the resonance forms (type B or D) in which the lone pair is located on only one germanium atom. In other words, the reaction of **1** with **7** provides strong support for the notion that the Ge—Ge double bond-resonating lone pair models B and D make a large contribution to the bonding in **1**.

The resonance forms represented by the dipolar structures B and D result in a charge separation. However, the M—M bond is homonuclear and is formally nonpolar which suggests that the singlet diradical form E may be significant. In essence, the trans-bending of a linear structure weakens the electron coupling in one of the π -bonds. This possibility was first raised by Popelier and coworkers³⁴ and is supported by our computational data where significant diradical character is calculated for the germanium model species MeGeGeMe .³⁵ For MeSnSnMe , the calculated energy minimum has a more strongly bent geometry ($\text{Me—Sn—Sn} = 100.0^\circ$) and much less diradical character than its germanium analogue.³⁵ These calculations on simple model species thus offer a straightforward explanation for the differences in reactivity that is based on diradical character.

(37) Takagi, N.; Nagase, S. *Organometallics* **2001**, *20*, 5498.

(38) Power, P. P. *Dalton Trans.* **1998**, 2939.

(39) Cui, C.; Spikes, G.; Power, P. P., unpublished work.

(40) An illustration of this phenomenon is provided by the effect of alkyl and amide substitution as shown by the monomeric structure of $[\text{Sn}\{\text{N}(\text{SiMe}_3)_2\}_2]_2$ ²² and the dimeric structure of $[\text{Sn}\{\text{CH}(\text{SiMe}_3)_2\}_2]_2$ ¹. The $-\text{N}(\text{SiMe}_3)_2$ and $-\text{CH}(\text{SiMe}_3)_2$ ligands are isoelectronic and have a very similar size, yet a monomeric structure is observed for the amide substituted compound.

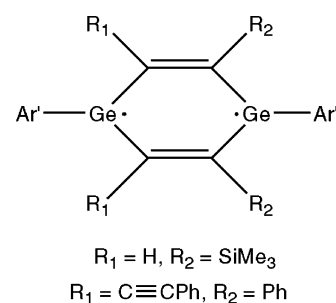
If, however, the experimentally observed bending angle ($125.24(7)^\circ$) and Sn–Sn bond length ($2.6675(4)$ Å) in **2** is assumed for MeSnSnMe, its diradical character is calculated³⁵ to be similar to that of MeGeGeMe, which suggests that the reactivity of **1** and **2** should also be similar. However, the calculations also show that the tin compound has a quite flat potential surface where the difference in energy between the calculated and experimentally found trans-bent geometries is less than ca. 5 kcal mol^{-1} . In other words, changing the bending angle and the SnSn distance in the tin species costs little energy. This leads to the conclusion that the geometry (and electronic structure) of **2** in solution may differ considerably from what it is in the crystalline state where crystal forces may affect the geometry. This is consistent with the previous results of Nagase³⁷ for germanium and tin compounds and those of Frenking for lead derivatives.³² In addition, it is consistent with the electrochemical behavior and the structure¹⁵ of the reduced species $[\text{Ar}'\text{SnSnAr}]^-$ as discussed above.

Experimental support for the diradical character of **1** comes from several of its reactions. For example, in its reaction with PhCN to produce **8**, two nitriles are coupled to produce the NC-(Ph)(Ph)CN moiety. In effect, a two-electron reductive coupling has occurred which is accompanied by a change in the formal oxidation states of the germaniums from +1 to +2. Both two-electron and four-electron reductive coupling by transition metal complexes to give diimino $^{-1}\text{N}=\text{C}(\text{R})-\text{C}(\text{R})=\text{N}^{-1}$ (as above) or enediimido $^{2-}\text{N}=\text{C}(\text{R})=\text{C}(\text{R})=\text{N}^{2-}$ products are known, although the mechanism of such coupling has received scant attention.⁴¹ Recent work by Cummins and co-workers, however, has suggested that coupling of nitrile to give the diimino product proceeds by initial one-electron reduction followed by dimerization of the radical thus generated to afford the C–C bonded species.⁴² Although no investigation of the mechanism of the reaction of **1** with PhCN has been performed, the previous work suggests that a one-electron reduction (by a loosely coupled electron at each germanium in **1**) of two benzonitriles followed by C–C bond formation is a plausible scheme for the generation of **8**. The observation of three different types of bridging ligand in **8** from the reaction of **1** with $\text{N}_2\text{CH}(\text{SiMe}_3)$, and the μ_2 -peroxo bridged structure for **10** are also consistent with the involvement of radicals in these reactions. The reaction of **1** with N_2O to produce the peroxo species **10** is notable because the known $\mu_2\text{:}\eta^2$ peroxo derivatives of Si, Ge, or Sn are derived from dioxygen in which the O–O bond is already formed.^{31a,43} In contrast, the reaction of low valent Si, Ge, or Sn with N_2O affords μ -oxo products. The observation of μ -O–O moieties derived from a source containing just one oxygen (N_2O) provides evidence for a reductive coupling reaction in which two N_2O molecules each are reduced by one electron with subsequent coupling to form the O–O bond.

The involvement of diradicaloid structures in the germanium derivatives obtained from **1** is also noteworthy. Thus, the reaction of **1** with N_3SiMe_3 gives the Ge_2N_2 ring compound **5**.

The diradicaloid character of this molecule is supported by its structural and spectroscopic properties and by calculations as previously described.¹⁷ In contrast, the reaction of N_3SiMe_3 with **2** gives the unique imido bridged species **6**. Reaction of **2** with a second N_3SiMe_3 ligand is not observed even with a large excess of N_3SiMe_3 . The reactions of **1** and **2** with N_3SiMe_3 provide a particularly striking illustration of the different reactivity of the tin and germanium species. This is especially true in light of the fact that a diradicaloid tin compound, $\text{ClSn}\{\mu_2\text{-N}(\text{SiMe}_3)\}_2\text{SnCl}$, related to **5**, can be synthesized by a different method.⁴⁴ It seems probable that the generation of **5** and **6** proceeds through different pathways that have their origin in the diradicaloid character of **1** although the details of either pathway remain unclear.

The activation of one of the flanking aryl groups in products **13** and **14** (eq 8) is notable and is consistent with the presence of a diradicaloid intermediate in the reaction. In this case, treatment of **1** with less hindered alkynes such as $\text{Me}_3\text{SiC}\equiv\text{CH}$ or $\text{PhC}\equiv\text{C}-\text{C}\equiv\text{CPh}$ produces the six-membered ring intermediates as shown by the structure:



Formally, this ring has six π -electrons, but instead of being stable and aromatic, it may have considerable diradicaloid character as illustrated above. It is probable that this form is sufficiently important to induce activation of one of the flanking $\text{C}_6\text{H}_3\text{-2,6-Pr}_2$ rings and afford the products **13** or **14** in moderate yield. The significance of diradicaloid structures in the reactivity of several classes of main group compounds is beginning to be recognized, and the behavior of **1** gives further support to the widespread nature of this phenomenon.⁴⁵ The regioselectivity of the reactions that produce **13** or **14** is also notable. We believe that this is an electronic effect of the SiMe_3 or Ph substituents which cause the closest germanium (in a putative intermediate analogous to **12**) to be more electrophilic (due to a flatter geometry) and thus more reactive toward the more electron rich carbon (carrying SiMe_3 or Ph) of the second equivalent of alkyne.

The reaction of **1** with TCNE was performed to investigate the oxidation behavior of **1**. Both **1** and **2** displayed irreversible oxidation waves in their cyclic voltammograms,¹⁴ and it was hoped that a 1:1 reaction of either **1** or **2** with TCNE would provide oxidized products containing an $[\text{Ar}'\text{EEAr}']^+$ moiety. For **1**, the unusual complex **11** in which three TCNE molecules oxidize two $\text{Ar}'\text{GeGeAr}'$ molecules to afford the fused ring structure illustrated in Figure 7 was obtained. The formal oxidation state of +1 for the four germanium atoms in 2 equiv of **1** become converted to one Ge^{4+} and three Ge^{2+} in **11**. The

- (41) Kukushkin, V. Y.; Pombeiro, A. J. L. *Chem. Rev.* **2002**, *102*, 1771. Cotton, F. A.; Hall, W. T. *J. Am. Chem. Soc.* **1979**, *101*, 5094. Esjornson, D.; Fanwick, P. E.; Walton, R. A. *Inorg. Chem.* **1988**, *27*, 3066.
 (42) Tsai, Y.-C.; Stephens, F. H.; Meyer, K.; Mendiratta, A.; Gheorghui, M. D.; Cummins, C. C. *Organometallics* **2003**, *22*, 2902. Mendiratta, A.; Cummins, C. C.; Kryatova, O. P.; Rybak-Akimova, E. V.; McDonough, J. E.; Hoff, C. D. *Inorg. Chem.* **2003**, *42*, 8621.
 (43) Cardin, C. J.; Cardin, D. J.; Devereux, M. M.; Convery, M. A. *Chem. Commun.* **1990**, 1461.

- (44) Cox, H.; Hitchcock, P. B.; Lappert, M. F. Pierssens, L. J.-M. *Angew. Chem., Int. Ed.* **2004**, *43*, 4500.

- (45) Grützmacher, H.; Breher, F. *Angew. Chem., Int. Ed.* **2002**, *41*, 4006.

mechanism whereby **11** is formed is unknown, although it seems probable that the reaction begins with a single electron transfer from a molecule of **1** to a cyano group of TCNE. Transfer of a further electron from the other germanium atom of **1** may then occur to give the compound $\text{Ar}'\text{GeNCC}(\text{CN})(\text{CN})\text{CCNGeAr}'$ in which two of the four cyano groups from TCNE carry an $\text{Ar}'\text{Ge}$ substituent. This is the product that we expected from the reaction. However, this species can apparently associate through cyanide bridging (as the structure of **11** suggests) and is also susceptible to oxidation by a further molecule of TCNE to give the unusual product **11**.

Finally, we draw attention to the fact that the lower reactivity displayed by **2** offers little support for significant diradical character. We have accounted for this behavior in terms of a solution structure for **2** that has a more strongly bent geometry and a longer Sn—Sn bond. In other words, it is a structure that is closer to C than it is to B, D or E and it has increased lone pair character at each tin. This proposal is supported by previously published experimental work on the one-electron reduction of **2**^{14,15} and theoretical calculations.^{35,37} Perhaps the best illustration of the increased bending is provided by the lack of reaction between **2** and CNBu' . Even with the more open

structure that results from the larger size of the metal, the CNBu' cannot interact with the tins to afford a product analogous to **7** because of the increased lone pair density caused by the greater bending in solution. The synthesis and characterization of RSnSnR molecules that display more strongly bent conformations in the solid state than that seen in **2** are underway.

Conclusions

The experimental data for the reactions of **1** and **2** with a variety of unsaturated molecules disclose a large difference in their reactivity. The lower reactivity of **2** is contrary to what is expected on the basis of bond energies and ionic or steric factors. The high reactivity of **1** is due to its singlet diradical character, a conclusion that is also supported by computational data.

Acknowledgment. We are grateful to the National Science Foundation for financial support.

Supporting Information Available: X-ray data for compounds **3**, **4**, **6**, **7**, **8**, **9**, **10**, **11**, and **14**. This material is available free of charge via the Internet at <http://pubs.acs.org>.

JA055372S